Techniques for simulating radiative transfer through porous media

Rich Townsend
Bartol Research Institute, University of Delaware, Newark, DE 19716, USA

In this contribution, I discuss some basic techniques that can be used to simulate radiative transfer through porous media. As specific examples, I consider scattering transfer through a clumped slab, and X-ray emission line formation in a clumped wind.

1 Introduction

A porous medium is one that is macroclumped: the typical scale of the clumps is larger than the mean free path $\bar{\ell}$ of photons. This represents the opposite end of the 'clumping spectrum' to a microclumped medium, for which the clump scale is smaller than $\bar{\ell}$. The distinction between these two limits is more than academic; although microclumping usually only affects the volume emissivity of a medium (which depends on the local density squared), porosity/macroclumping can result in the medium having an effective opacity κ_{eff} that is significantly smaller than the microscopic value κ of the material comprising it.

Recent investigations of porosity (e.g., Oskinova, Feldmeier & Hamann 2004; Owocki & Cohen 2006) have been focused primarily toward evaluating its observable consequences. As such, these studies have relied largely on very simple models for the radiative transfer. In this contribution, I discuss some of the basic techniques and codes that I have devised to move beyond these simplified models, allowing consideration of the full radiative transfer problem for a clumped medium.

The standard approach to radiative transfer is to solve the radiative transfer equation (RTE),

$$\frac{\mathrm{d}I}{\mathrm{d}\tau} = I - S, \tag{1}$$

where I is the specific intensity, S the source function, and τ the optical depth coordinate. However, solving the RTE is not the only way to tackle the problem. Instead of the I-based 'field' approach embodied by the RTE, one can adopt a 'particle' approach, following individual photons as they propagate through a medium. This is precisely what Monte-Carlo radiative transfer entails, and in the following section I apply this approach to model scattering transfer through a clumped slab.

2 A clumped scattering slab

To investigate radiative transfer in a clumped scattering medium, I have developed FREYR, a Monte-Carlo code for simulating the propagation of photons through a plane-parallel slab composed of discrete, spherical clumps. The clumps are randomly positioned, but each has the same radius r_{c} and a uniform density ρ_{c}. Photons are introduced at the bottom of the slab with a random upward direction. A nominal 'optical distance to travel' τ is assigned to each photon based on the expression

$$\tau = -\log x, \tag{2}$$

where x is a uniform random deviate in the range $0 < x \leq 1$. This optical distance is converted into a physical distance ℓ by inverting the optical depth equation

$$\tau = \int_0^\ell \kappa \rho(\ell')\,\mathrm{d}\ell'; \tag{3}$$

here, the microscopic opacity κ is assumed to be constant, while the local density ρ varies with position as the photon passes in and out of spheres. After moving a distance ℓ in the appropriate direction, the photon is scattered: a new random direction is chosen (corresponding to isotropic scattering), and a new optical distance is picked using eqn. (2). This procedure is repeated until the photon escapes from the top or the bottom of the slab; periodic boundary conditions are applied at the sides of the slab.

Conceptually, this procedure is quite straightforward; but from an implementation perspective the tricky part comes in inverting the optical depth equation (3). The key to this task lies in the recognition that along any given ray through the slab, the density is a piecewise-constant function. Changes in ρ arise only at those discrete points where the ray enters or exits a sphere. To locate these points, the parametric equation for the ray traversed by a photon is written as
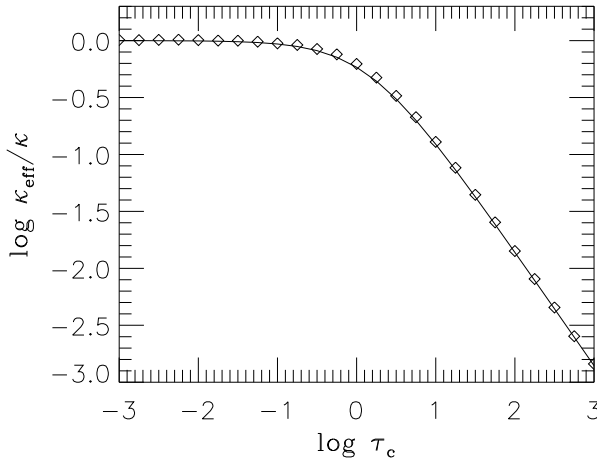
$$\mathbf{r} = \mathbf{r}_0 + \ell\mathbf{dr}. \tag{4}$$

Figure 1: The ratio between the effective opacity κ_{eff} and the microscopic opacity κ, plotted (diamonds) as a function of clump optical thickness τ_{c}. The solid line shows the corresponding prediction of the simple bridging law (14).

Here, $\mathbf{r}_0$ is the starting position vector of the photon, and the unit vector $\mathbf{dr}$ gives the photon's direction. To establish whether this ray intersects a sphere located at $\mathbf{r}_{\text{s}}$, FREYR calculates the following quantities:

$$\mathbf{v} = \mathbf{r}_0 - \mathbf{r}_{\text{s}} \qquad (5)$$

$$B = 2\mathbf{dr} \cdot \mathbf{v} \qquad (6)$$

$$C = \mathbf{v} \cdot \mathbf{v} - r_{\text{c}}^2 \qquad (7)$$

$$D = B^2 - 4C \qquad (8)$$

If $D > 0$, then the ray pierces the sphere at the locations

$$\ell_{\text{s}} = \frac{-B \pm \sqrt{D}}{2}; \qquad (9)$$

these correspond to the points where the density undergoes a jump. Between these points, ρ is constant, and τ varies linearly – so it is straightforward to reconstruct the function $\tau(\ell)$ from eqn. (3), and then to invert this function to find ℓ given τ.

For each leg of a photon's journey, the ray-sphere intersection test (5–9) must be performed against *every* sphere contained in the slab. Potentially, this can be quite time consuming, and so FREYR uses a spatial partitioning approach to reduce the number of tests that must be done. After the distribution of spheres is calculated (i.e., a set $\{\mathbf{r}_{\text{s}}\}$ of random centers), the slab is divided up into a 3-dimensional array of voxels. Each voxel stores a index list of those spheres that fall part or all of the way inside it. To find out which spheres a ray intersects, it is then

only necessary to test the subset of spheres that are indexed by the voxels that the ray passes through. Efficient algorithms exist (e.g., Amanatides & Woo 1987) for quickly finding these voxels.

Having described the basic principles of FREYR, let me now present some illustrative results. Fig. 1 plots the ratio $\kappa_{\text{eff}}/\kappa$ between the effective and microscopic opacities of a clumped slab, as a function of the averaged clump optical thickness

$$\tau_{\text{c}} = \frac{4\kappa\rho_{\text{c}}r_{\text{c}}}{3}. \qquad (10)$$

To obtain the κ_{eff} datum at each τ_{c} abscissa, a FREYR simulation is used to determine an empirical value for the slab transmittance

$$T \equiv \frac{N_{\text{esc}}}{N_{\text{inj}}}; \qquad (11)$$

here, N_{inj} is the number of photons injected at the bottom of the slab during the simulation, and N_{esc} is the number that eventually escape through the top. Formally, the transmittance is a function only of the slab optical thickness, so that

$$T = f(\kappa_{\text{eff}}\bar{\rho}\Delta z) \qquad (12)$$

for some function $f()$. Thus, armed with the empirically-measured value of T, and the known values of the slab mean density $\bar{\rho}$ and vertical extent Δz, the effective opacity follows as

$$\kappa_{\text{eff}} = \frac{f^{-1}(T)}{\bar{\rho}\Delta z}. \qquad (13)$$

The only difficulty is to determine the inverse of the transmittance function, $f^{-1}()$, but this can be done numerically using Monte-Carlo simulations of a homogeneous, isotropically scattering slab.

Looking at Fig. 1, the onset of porosity is plain to see. Once the clumps become optically thick (i.e., $\tau_{\text{c}} > 1$), the effective opacity of the slab begins to fall well below the microscopic value κ. This drop-off is well approximated by

$$\frac{\kappa_{\text{eff}}}{\kappa} = \frac{C}{C + \tau_{\text{c}}} \qquad (14)$$

(shown in the figure by the solid line), where the constant $C \approx 1.4$. This expression is a modified form of the bridging law introduced by Cohen & Owocki (2006). In the limit of small τ_{c}, it correctly reproduces the microclumping case, for which κ_{eff} equals the microscopic opacity κ. In the opposite limit of large τ_{c} (i.e., macroclumping), the effective opacity has a scaling

$$\kappa_{\text{eff}} = \frac{\kappa C}{\tau_{\text{c}}} = \frac{3C}{4\rho_{\text{c}}r_{\text{c}}}. \qquad (15)$$

Multiplying through by the clump mass $4\pi\rho_{\text{c}}r_{\text{c}}^3/3$ then gives the effective cross section of the clumps,
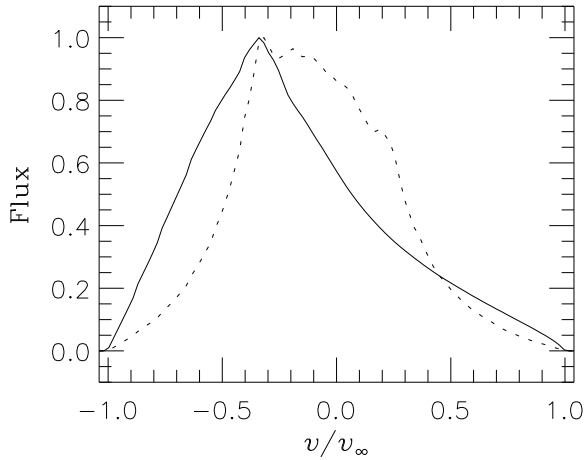
Figure 2: X-ray line profiles for a $\tau_* = 3$ clumped wind. The solid (dotted) profile corresponds to optically thin (optically thick) clumps; both profiles are normalized to have a maximum flux of unity.

$$\sigma_{\text{eff}} = C\pi r_{\text{c}}^2. \tag{16}$$

This can be recognized as the geometric cross section πr_{c}^2, scaled by the constant C. The basis for this result is that the clumps – when they become extremely optically thick – behave like individual scattering centers, with an interaction cross section equal to their geometric cross section. The appearance of the constant C is to correct for the angular scattering profile of each individual clump. If this profile were isotropic, then we would obtain $C = 1$; but in fact the profile is that of a sphere with a Lambert-law surface (see Schoenberg 1929), leading to the 'observed' value $C = 13/9 \approx 1.4$.

3 A clumped absorbing wind

The utility of Monte-Carlo is that it works in cases such as scattering where the source function S is difficult to obtain. If in fact S is already available, then a simple formal solution of the RTE (cf. eqn. 1) is

$$I = \int S e^{-\tau} \mathrm{d}\tau. \tag{17}$$

Calculating the intensity I using this expression is invariably faster than performing an equivalent Monte-Carlo simulation. (This is a specific instance of a general rule: *Monte-Carlo is guaranteed to be the slowest way to solve a radiative transfer problem.* Of course, sometimes – as with scattering – it is the only straightforward way.)

The calculation of X-ray emission line profiles in clumped winds (see, e.g., the contribution by David Cohen) is a specific example of a case where the formal solution (17) can be used. X-ray line photons are emitted according to some simple parametric function of radius, meaning that the source function is easy to calculate. These photons are then re-absorbed by an opacity associated with a distribution of clumps. As with the Monte-Carlo simulations, the tricky part in modeling this re-absorption involves evaluating the optical depth τ.

Fortunately, for spherical clumps the same set of techniques (cf. §2) can be applied. If the inter-clump medium is a vacuum, then once again the density along any given ray is a piecewise-continuous function, and the ray-sphere intersection testing (cf. eqns. 5–9) can be used to reconstruct $\tau(\ell)$. If, more realistically, there is a smooth inter-clump medium following a wind expansion law $\rho = \dot{M}/(4\pi r^2 v)$, then the contribution of this medium to the optical depth along a ray can be added in using numerical quadrature.

Fig. 2 shows some example X-ray line profiles calculated using BOREAS, a simple formal solver for a spherical-clump wind. For both profiles, the optical depth τ_* to the star (cf. Owocki & Cohen 2006) is 3; however, the profiles differ in the nature of the clumping. The solid-line profile is for a configuration composed of many optically thin clumps, and it shows the characteristic asymmetric (blue-skewed) shape usually associated with a smooth wind. Conversely, the dotted-line profile is for a configuration composed of fewer, optically thick clumps. With porosity acting to reduce the effective opacity of the wind, a much more symmetric line profile is seen in this latter case.

4 Summary

The spherical clumps considered herein admittedly rather idealized. However, it is precisely for such simple, idealized cases that one can hope to fully understand the precise manner in which porosity modifies the effective opacity of a medium. Both FREYR and BOREAS – and the techniques they implement – will certainly prove useful in developing such an understanding.

References

Amanatides, J., & Woo, A. 1987, in *Eurographics '87*, p. 3

Owocki, S.P., Cohen, D.H. 2006, *ApJ*, **648**, 565

Oskinova, L.M., Feldmeier, A., & Hamann, W.-R. 2004, *A&A*, **422**, 675

Schoenberg, E. 1929, *Handb. Astro.*, **2**, 255